



Orange2022

Design Report

Kimihito Mori

kimihito.mori.4k@stu.hosei.ac.jp

Yuta Fujimori

yuta.fujimori.4b@stu.hosei.ac.jp

Koki Kubota

koki.kubota.8p@stu.hosei.ac.jp

Shunki Shibuya

shunki.shibuya.5v@stu.hosei.ac.jp

Riki Uchida

riki.uchida.6f@stu.hosei.ac.jp

Faculty Advisor Statement

I hereby certify that the engineering design on Orange2022 was done by the current student team, and it is significant and equivalent to what might be awarded credit in a senior design course.

Signed

Date

Handwritten signature of Kazuyuki Kobayashi

Handwritten date May 12, 2022

Prof. Kazuyuki Kobayashi

May 12, 2022

Professor Kazuyuki Kobayashi

Assistant Professor Tomoyuki Ohkubo

Faculty of Science and Engineering, Hosei University

3-7-2 Kajinocho Koganei, Tokyo 184-8584, Japan

E-mail; ikko@hosei.ac.jp

1. Introduction

The Hosei University Autonomous Robotics Laboratory (ARL) team is proud to present a newly designed vehicle, Orange2022. This vehicle is updated as per the rules and guidelines of IGVC2022 and differs substantially from the vehicle used for participation in IGVC2019. The significant differences between the rules of IGVC2022 and IGVC2019 are summarized in Table 1.

Table 1. Differences in rules of IGVC2019 and IGVC2022

Rules	IGVC2019	IGVC2022
Course	Grass area	Asphalt pavement
Course wide	100 feet	140 feet
Course deep	200 feet	120 feet
Course long	600 feet	450 feet
Outer boundaries	Painted on the grass	Taped on the asphalt
Total distance	10 minute mark	5 minute mark of runtime
Disqualify vehicle		Degrades the course

Through team discussions, it was established that significant changes in the vehicle design were required due to changes in the driving course and environment from grass to asphalt pavement, and the course time for the total distance is reduced from 10 min to 5 min. This means that the vehicle requires faster navigation speed with running stability. Moreover, the vehicle must be carried from Japan by air. This warranted additional requirements for our vehicle design, which are summarized in Table 2.

Table 2. Requirements for IGVC2022 and carrying from Japan

IGVC2022 rules	Expected Requirement
Asphalt pavement	Faster running with stability
5 minute mark of runtime	
Taped on the asphalt	Optimize lane recognition algorithm for Tape
Airline rules carrying from Japan	Expected Requirement
The size of the baggage must not exceed 62 inches in length × wide × height	The vehicle must be designed for easy disassembly and must be carried in suitcases

The hardware design was reviewed, and the software was modified and recalibrated to achieve a vehicle that meets these requirements. The hardware design included new elements, such as the introduction of a folding mechanism to change the aspect ratio of the vehicle body and a new suspension to withstand increased speeds while maintaining stability and avoiding tipping on sharp curves.

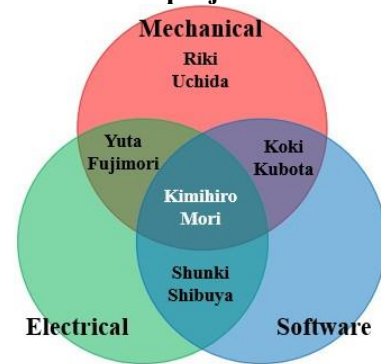
1.1 Team organization

This year's ARL team comprised five graduate student members. The ARL team was organized into mechanical, electrical, and software sub-teams. This enabled specialized focus on specific design areas. Table 3 summarizes the roles assigned and the time spent for each sub-team. Each member was assigned an appropriately overlapping sub-team role based on their design skills to

facilitate communication among team members.

Table 3. Roles of individuals and hours spent by them on the project

Team Member	Areas of Concentration			Hours
	Mechanical	Electrical	Software	
Kimihito Mori (Team Leader)	○	○	○	700
Koki Kubota	○		○	600
Shunki Shibuya		○	○	600
Yuta Fujimori	○	○		600
Riki Uchida	○			100



1.2. Design process

The goal of the ARL team was to complete faster navigation in the IGVC2022 autonomous course without failure. Our team used a V-shaped waterfall development model as the development methodology for mechanical, electrical, and software aspects to achieve this goal. Figure 1 illustrates the design process using a V-shaped model of waterfall development.

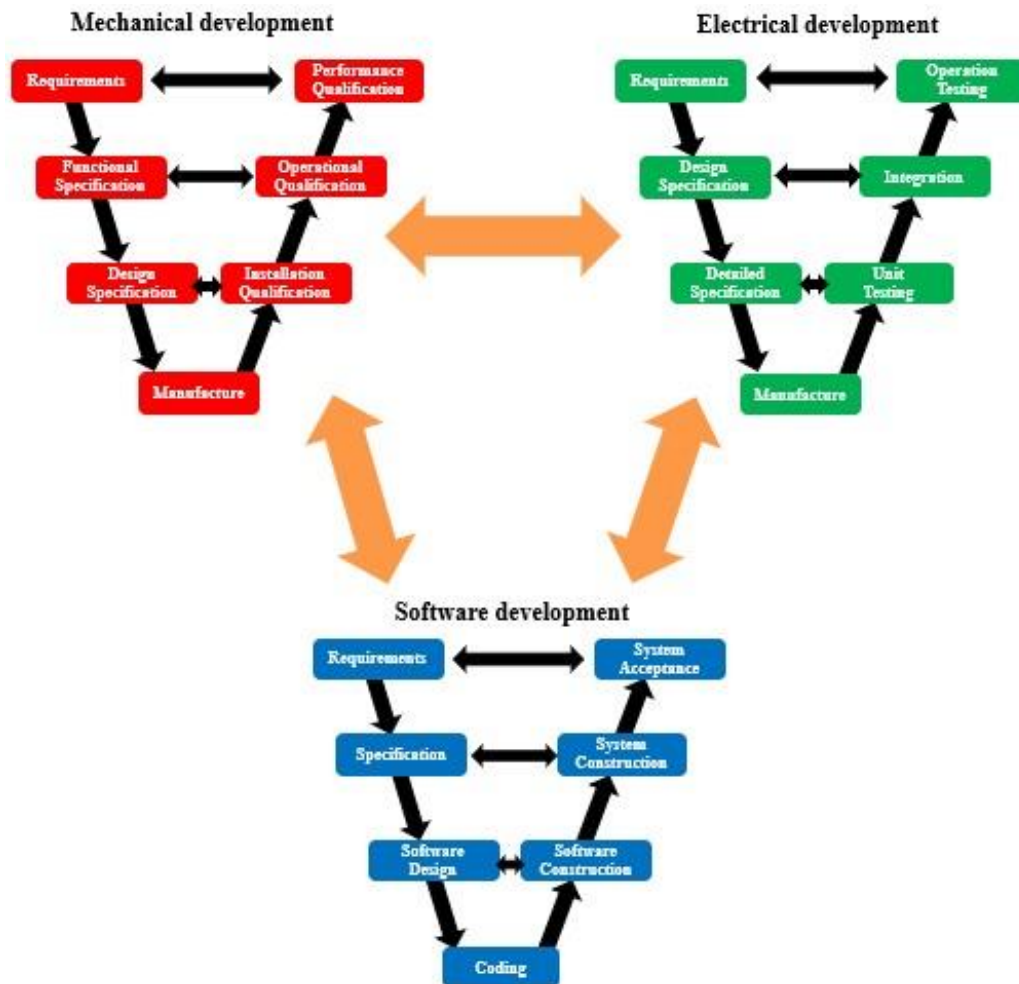


Figure 1. Our development processes

In this development approach, defects were detected early in the design and checking stages. Additionally, the quality of the developed mechanical, electrical, and software systems was improved by verifying and checking the developed system by other design group members.

2. Innovations

This section summarizes various innovations, including mechanical, electrical, and software innovations, in vehicle design. Table 4 summarizes the design issues and innovative improvements.

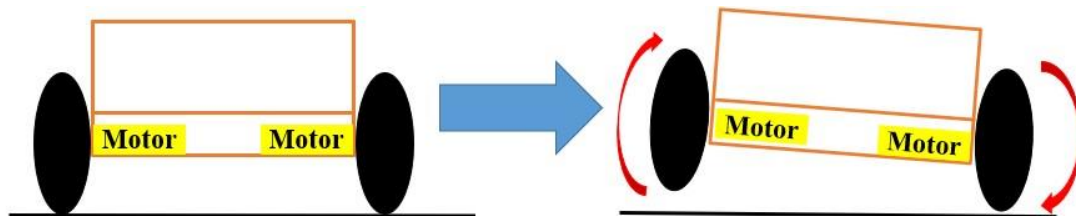
Table 4. Hardware and software improvement

Subgroups	Problem	Improvement
Mechanical	Navigating at relatively high speed on a curvy course may result in tipping	Introduction of suspension mechanism to prevent tipping
	Carrying size problem	A new folding frame was introduced in the design of the vehicle frame to match the size of the suitcases
Electrical	Low resolution problem for Omnidirectional camera	Employ new omni-directional camera
	Motor driver heat dissipation problem due to unexpected higher load such as climbing lamp	Consider employing a heat sink and positioning the motor driver to account for ambient air flow
Software	OS and ROS software upgrades due to end of support	Apply the virtual container method using Docker to achieve seamless upgrades

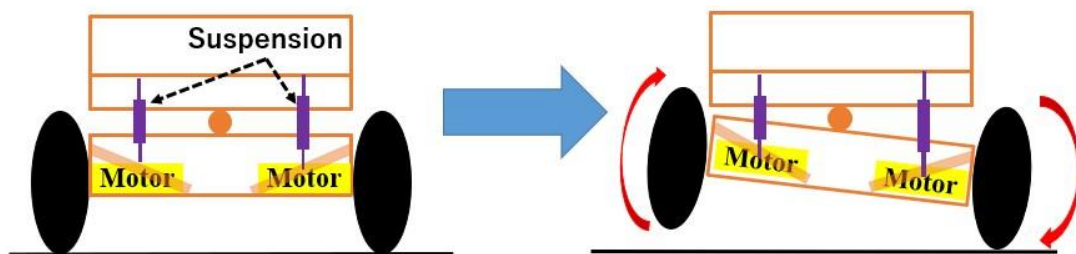
2.1. Hardware design

2.1.1. Employment of suspension to stability

Based on the difference in rules between IGVC2019 and IGVC2022, the running field is now asphalt, which is expected to increase the average speed of the vehicles. Hence, it is critical to address vibrations in the left-right directions than those in the up-down directions.



(a) Orange2019



(b) Orange2022

Figure 2. (a) Orange2019 and (b) Orange2022

Figure 2(a) shows the basic mechanical structure of the connection between the motor and chassis in Orange2019. As the motor and chassis were directly connected, vibration of the entire vehicle was a major problem. As shown in Figure 2(b), a rigid axle suspension was introduced around the vehicle's front wheels to press the wheels against the road surface and reduce the impact transmitted to the vehicle. This prevented vibrational problems and was adapted to the asphalt track, thereby improving stability.

2.1.2. Foldable framework

As shown in Figure 3, a folding mechanism was employed for the new vehicle design to satisfy both the requirements of running stability and carrying the vehicle in a suitcase.

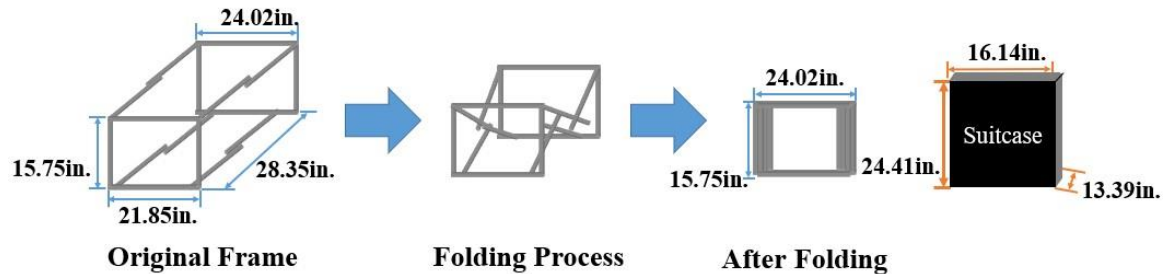


Figure 3. Foldable frame of Orange2022

2.1.3. Stable lanes and obstacles recognition at a faster frame rate

With changes in the IGVC rules and guidelines, the autonav course changed from a grassy area to asphalt pavement. To achieve stable high-speed navigation in such an environment, a more comprehensive range and higher image resolution of peripheral vision are required. Therefore, we employed an Insta360 camera instead of a conventional Theta S camera to satisfy these requirements. A comparison between the two cameras is presented in Table 5.

Table 5. Performance comparison between Theta S and Insta360

	Theta S 	Insta360 
Resolution	1280 × 720	2560 × 1280
Frame Rate	15fps	30fps
Weight	125g	26.5g

2.2. Motor control driver

Orange2019 experienced frequent motor driver failures during competitions. Upon examining the failed motor drivers, we found that multiple FETs were thermally damaged due to overcurrent. This was attributed to the fact that the motor driver was subjected to a more substantial load than expected while climbing a ramp during the competition. Although the motor driver should be able to withstand the expected current according to its specifications, the motor driver's heat sink was reinforced as a precaution to prevent the failure of the motor driver, as shown in Figure 4.

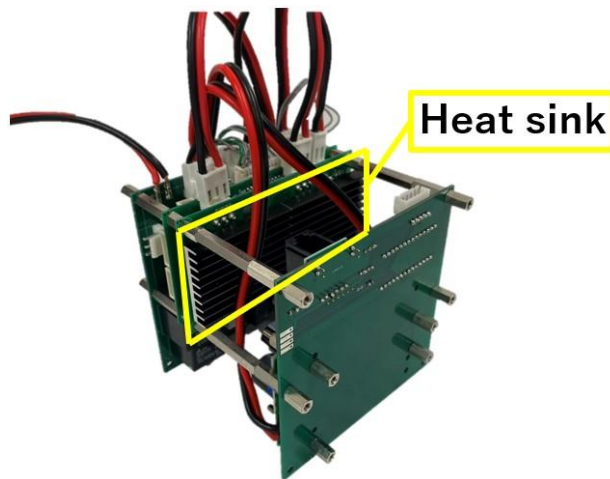


Figure 4. Motor driver with heat sink

2.3. Software design

Orange2019 used software with the open-source ROS kinetic on the OS Ubuntu 16.04. However, because Ubuntu 16.04 will be unsupported in May 2021, it was necessary to migrate to Ubuntu 20.04 with ROS noetic. To prevent reinstallation of the Ubuntu OS in the control computer, we applied a Docker-based virtual container approach to migrate the existing ROS kinetic control software to new ROS noetic control software with seamless migration. Consequently, only the latest Ubuntu OS and Docker were needed instead of installing two different ROS versions directly on the control computer. Using the latest Docker, the two ROS versions and the corresponding Ubuntu version of the OS could be implemented as individual virtual containers within Docker. By using "Dockerfile," consistent build container images were built quickly.

3. Mechanical Design

3.1. Design overview

Figure 5 shows an overview comparison of the Orange2019 and Orange2022 vehicle bodies, and Figure 6 shows the exterior materials employed.



(a) Orange2019 **(b) Orange2022**
Figure 5. The design comparison between the Orange2019 and Orange2022 vehicle body

The significant hardware difference between Orange2019 and Orange2022 is

(1) vehicle dimensions, (2) exterior of the vehicle, and (3) enhanced running stability.

(1) The dimensions of Orange2019 were limited by the size constraints of the suitcases used for transportation from Japan. However, the newly introduced folding mechanism enables the design of a vehicle that is larger than suitcases.

(2) Owing to the folding mechanism, the exterior was changed from plastic boards to waterproof cloth to reduce weight, as shown in Table 6, for ensuring that the fittings are easier to maintain in a sudden accident.

Table 6. Exterior weight comparison between the plastic board and waterproof cloth

	Plastic board	Waterproof cloth
		
Weight (g/m ²)	800	117.6

(3) We introduced a new suspension mechanism to prevent tipping when the vehicle runs on curves, which enhances its running stability.

3.2. Weight distribution

Weight distribution is essential for ensuring the running stability of a vehicle Table 7 lists the major heavy component weights of the vehicle and the weight ratios. As shown in Figure 6, relatively heavy components were designed to be allocated symmetrically to achieve running stability. For the competition, the competition payload location was reserved at a low position in the rear to prevent the weight distribution change and ensure that the center of gravity of the vehicle did not affect it significantly.

Table 7. Heavy components weight of the vehicle and weight ratios.

	Weight (pound)	Weight ratios (%)
Payload	20.0	19.8
Wheels	12.8	12.6
Batteries	12.4	12.3
Suspensions	4.0	3.9
DC/DC converter	3.7	3.7
Others	48.3	47.7
Total	101.2	100

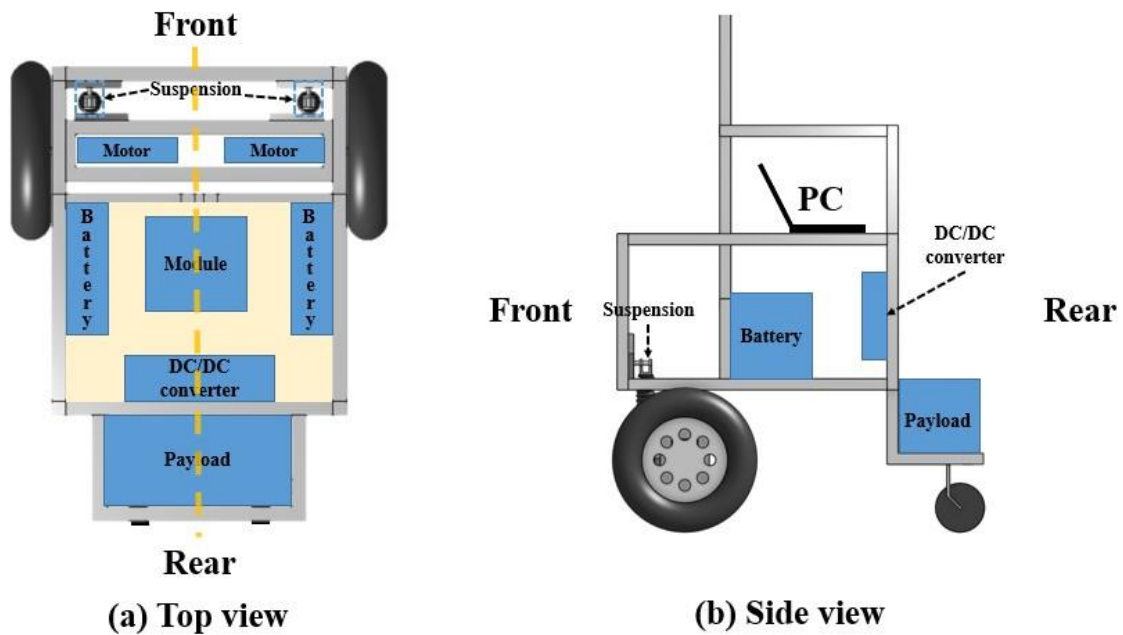


Figure 6. Various components of Orange2022

4. Electrical Design

According to IGVC rules, vehicle E-stops must be hardware-based and not controlled through software. As shown in Figure 7, the motor control driver, wired and wireless E-stop driver, and LED driver are integrated into one module to satisfy these requirements. Figure 8 shows the integrated vehicle control module. When the E-stop is pressed, the E-stop driver is activated. The current connection between the motor driver and motors is immediately disconnected and the vehicle is stopped. Simultaneously, the vehicle running state indication changes through the LED driver to indicate the E-stop state.

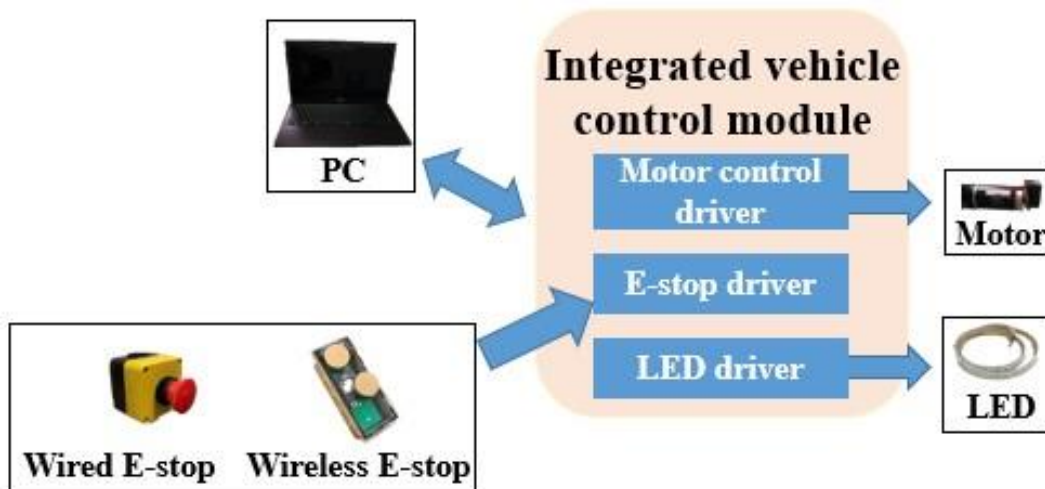


Figure 7. Configuration of developed integrated vehicle control module

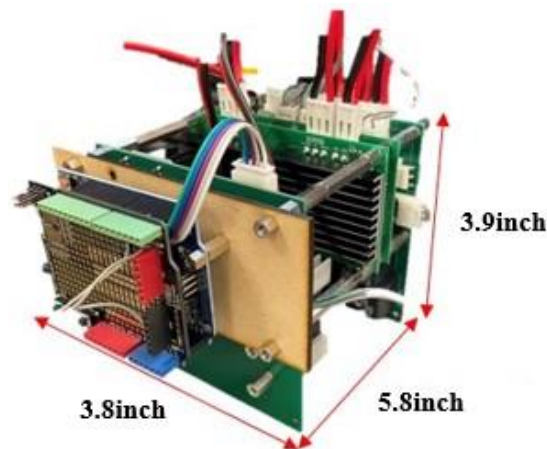


Figure 8. Developed integrated vehicle control module

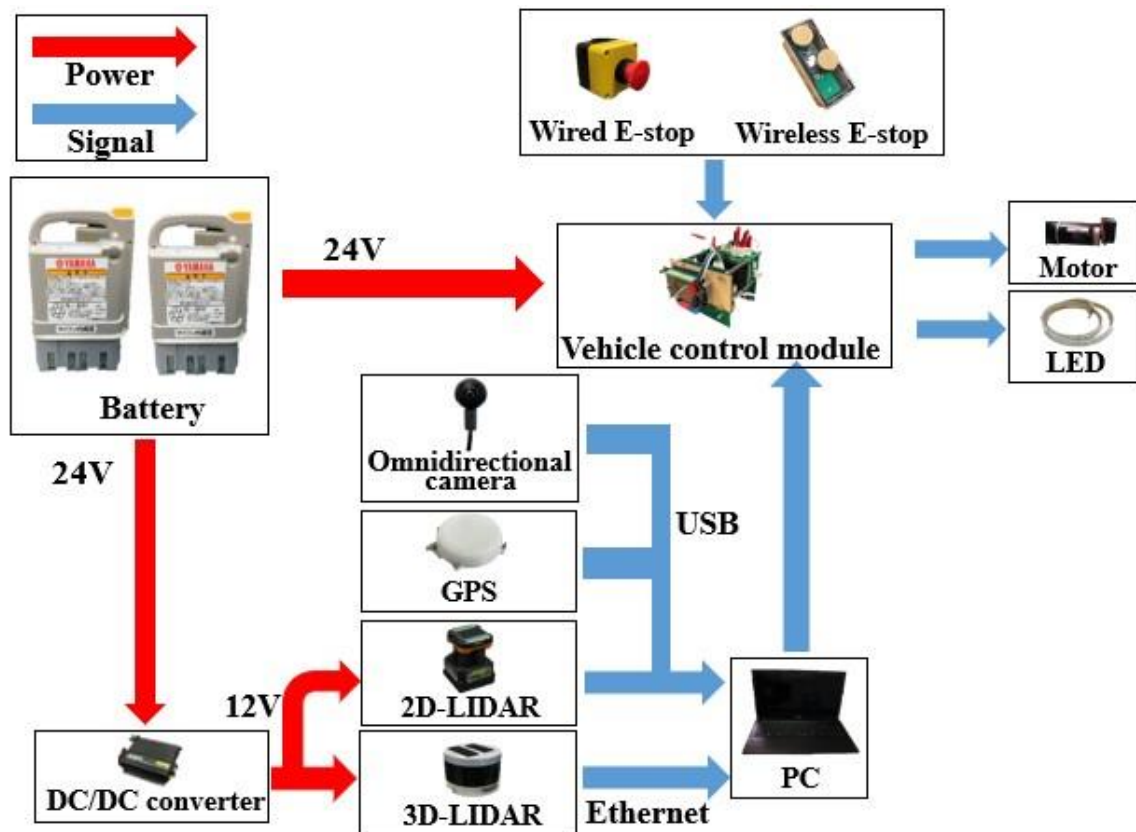


Figure 9. Power and signal flow of Orange2019

4.1 Power distribution system

Figure 9 shows the overall power distribution of Orange2022. Herein, the red and blue lines indicate the power and signals, respectively.

A significant difference in Orange2022 from Orange2019 is the dual-power supply configuration, as shown in Figure 8, by considering the power backup and weight distribution to prevent tipping.

A 24 V NiMH battery supplies power to the integrated vehicle control module. A 24–12 V DC/DC converter supplies power to onboard sensors, such as GPS, 3D-LIDAR, and 2D-LIDAR. The 2D-

LIDAR, omnidirectional camera, GPS, and integrated vehicle control module are connected to a laptop PC via USB and 3D-LIDAR via an Ethernet cable. Table 8 summarizes the electrical components in Orange2022.

Table 8. The Orange2022 electrical components

Component	Product name	Power Consumption	Operating Voltage	Source	Team cost (Retail cost)
3D-LIDAR	Velodyne LIDAR VLP-16	12W	12VDC	Power supply from DC/DC converter	\$11,685 (\$0)
2D-LIDAR	HOKUYO UTM-30LX	8W	12VDC	Power supply from DC/DC converter	\$4,000 (\$0)
GPS	NEO-M8P	—	12VDC	USB	\$220 (\$0)
Omnidirectional camera	Insta360	—	USB Power	PC	\$330 (\$0)
Laptop personal Computer	FRONTIER NX series	30W	19VDC	Power supply from DC/DC converter	\$840 (\$0)

●3D-LIDAR: This sensor collects the 3D shape of obstacles and 360° surrounding obstacles from 0.7 to 328 ft ahead with an accuracy of ± 0.1 ft. It is used for map generation and recognition of self-position localization of the vehicle.

●2D-LIDAR: This sensor covers the environments in the range of 180° in the horizontal direction, and it can measure from 0.3 to 98.4 ft distance ahead with an accuracy of ± 0.1 ft. It is used for obstacle detection.

●GPS: This GPS has an RTK correction function when RTK correction signals are available. It is used to recognize the self-position of the vehicle.

●Omnidirectional camera: This camera has dual-lens views and covers the upper and lower sides. The lower-side lens is used to detect the lane, whereas the upper-side lens is used to detect the ambient light intensity by which the lane detection threshold is determined.

4.2 Safety devices and system integration

Figure 10(a) and (b) show a wired and wireless E-stop, respectively. The wireless E-stop uses ZigBee; when the E-stop is pressed, the power supply from the integrated vehicle controller module to the motor can be immediately deactivated without any PC operation.



(a) Wired E-stop



(b) Wireless E-stop

Figure 10. (a) Wired E-stop, (b) wireless E-stop

As shown in Figure 11, the LED lights display red flashing as a warning mode during autonomous driving. When the E-stop is pressed, the power supply from the integrated vehicle controller module to the motor is disconnected. The LED lights are immediately displayed in blue as a safe mode.

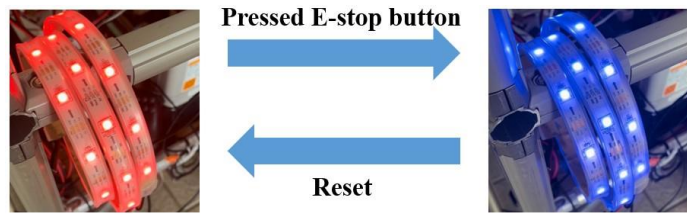


Figure 11. Mechanism of E-stop and LED light

5. Software Development

Orange2019 was developed using a combination of Ubuntu 16.04-ROS kinetic; however, we use the Docker container-based migration with the end of support for both the distribution version of Ubuntu and ROS approach to achieve migration to the Ubuntu 20.04-ROS noetic successfully. The implementation of each module is described as follows.

5.1 Obstacle detection and avoidance

Table 9 shows the sensors used for obstacle detection and their roles.

Table 9. Obstacle detection sensors and their roles

Component	Use applications
2D-LIDAR	Used for obstacle detection and avoidance and local map generation.
3D-LIDAR	Used to generate a global SLAM map
Omnidirectional camera	Used for map generation and local map generation

Orange2022 uses SLAM to generate global and local obstacle maps based on information from 2D-LIDAR, 3D-LIDAR, and omnidirectional cameras. Subsequently, these maps are used for navigation. Figure 12 shows the global and local obstacle maps generated by SLAM from data obtained from 2D-LIDAR, 3D-LIDAR, and omnidirectional cameras.

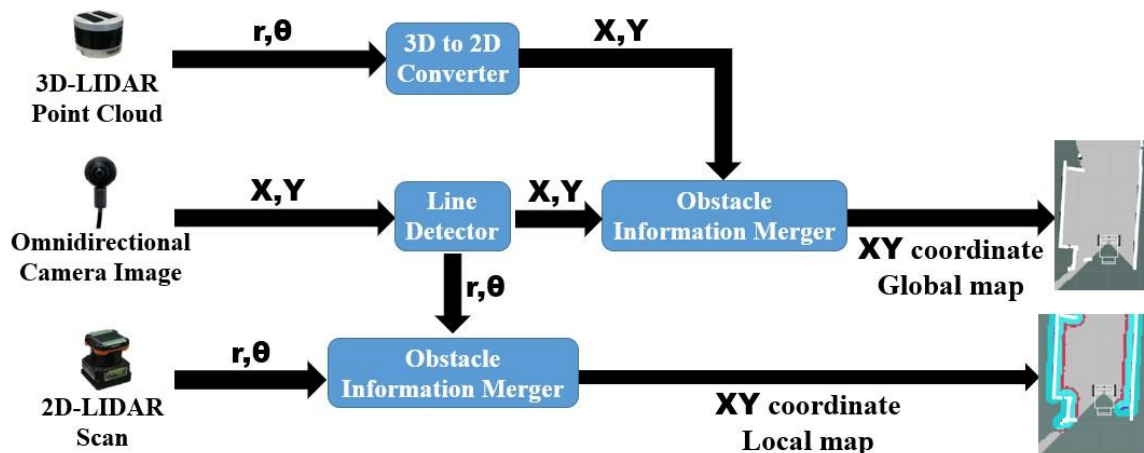


Figure 12. How to generate both local obstacle and global obstacle maps

5.2 Lane and simulated pothole detection as obstacles

Lanes and simulated potholes could not be detected using LIDAR. Therefore, as shown in Figure 13, the images obtained from the omnidirectional camera were converted to the r-theta 2D LIDAR coordinate frame and treated as obstacles observed by 2D LIDAR.

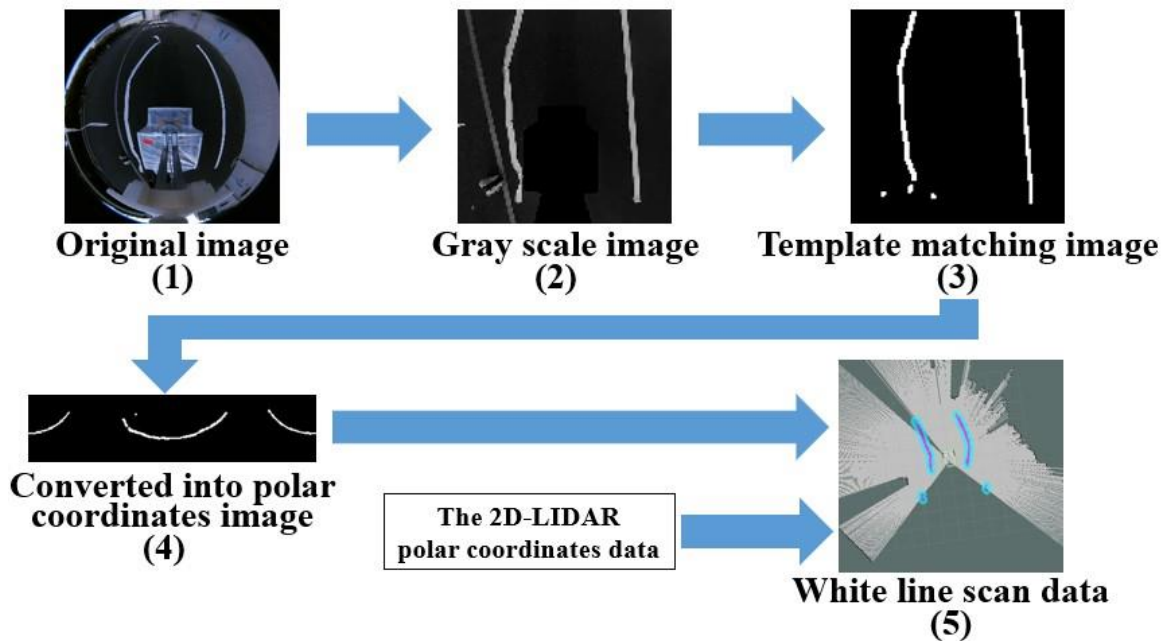


Figure 13. Lane recognition procedure

- (1) Grab images from an omnidirectional camera.
- (2) Convert the image acquired in (1) into a ground-plane image and convert it to grayscale.
- (3) Binarize the image by applying template matching to the image obtained in (2).
- (4) Convert the image obtained in (3) into an r-theta image for combination with 2D-LIDAR data.
- (5) Composite the image obtained in (4) with the data obtained by 2D-LIDAR.

The lanes recognized by the above-mentioned procedures are used as obstacles for navigation and are combined with obstacle data detected by 2D-LIDAR and 3D-LIDAR to analyze and avoid environmental conditions.

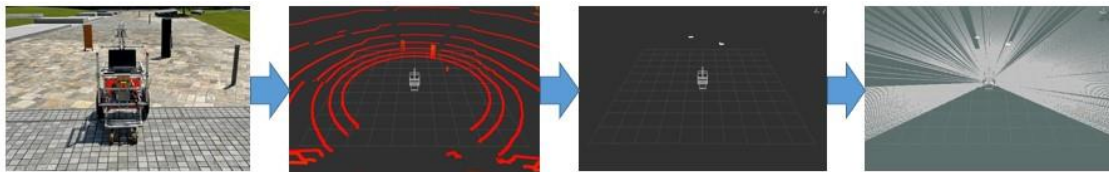
5.3 Self-localization and path planning

There are two methods for estimating self-position: using GPS or using the local obstacle map and global obstacle map generated by SLAM.

A potential field map is generated from the estimated self-position and global obstacle map for path planning. The path to the next waypoint is planned by iterating the path planning using the A-star algorithm for the local obstacle map obtained by 3D-LIDAR and the omnidirectional camera.

5.4 Local obstacle map generation from 3D-LIDAR

Figure 14 shows the flow of local obstacle map generation using 3D-LIDAR.



(a)View of the vehicle (b)The 3D image (c)The 2D image (d)The generated image

Figure 14. Typical example of the generated local obstacle map

Figure 14(a) shows the surrounding obstacles because the data obtained by 3D-LIDAR has a wider measurement range than the 2D-LIDAR employed. Figure 14(b) shows the surrounding obstacles detected by 3D-LIDAR, and Figure 14(c) shows the data obtained from 3D-LIDAR converted into a 2D image. The white dots represent obstacles. If the size of the obstacle differs between the top and bottom, the one closer to the vehicle is considered the size of the obstacle. Figure 14(d) shows the generated local obstacle map, wherein the light gray areas are the areas that can be traveled and the dark gray areas are the undetermined areas. The generated local obstacle map is saved even if navigation fails and only the map generated in the previous run is used. Because 3D-LIDAR cannot acquire information on obstacles in the vicinity, 2D-LIDAR is also used for driving.

5.5 Path planning to the goal

Path generation can be divided into cost maps and path planning. The cost map represents the risk of collision with obstacles and is generated based on the relative positions of the vehicle and obstacles. There are two types of cost maps: global and local maps. The global cost map uses information from the global map, whereas the local cost map uses navigation information from the local map.

The shortest path to the goal is calculated based on a cost map in path planning. There are two types of path planning: global and local path planning. Global path planning refers to the global cost map, whereas the local path planning refers to the local cost map.

Figure 15 shows how the path is generated. The purple, blue, and red colors indicate the object's location, the areas of possible collision with obstacles, and the boundary of the area to be avoided, respectively. The green line coming out from the front of the vehicle is the path generated by the global path planning, and the blue arrow is the path generated by the local path planning.

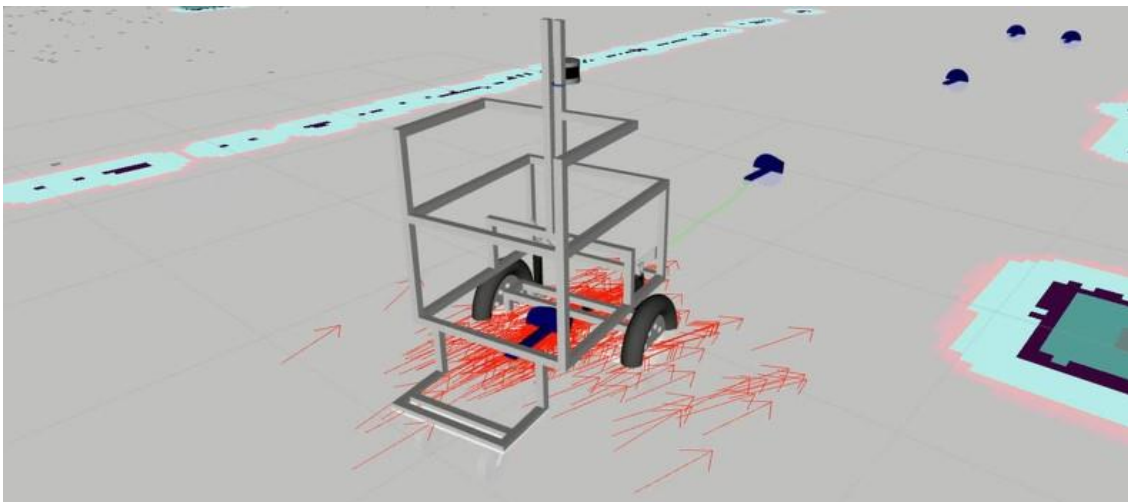


Figure 15. Path planning

6. Failure Points

Table 10 shows the expected vehicle failures and their solutions in Orange 2022.

Table 10. Vehicle failure points and resolutions

Problem	Solution
Frame breakage problem	Solved by use a general-purpose frame and to make it easy to replace the frame with a spare frame in the event of damage.
Sensor failure problem	Solved by making the onboard sensors in a redundant configuration and changing the sensor settings in the ROS launch file to maintain stable navigation.
Motor control module breakage problem	Solved by having a backup spare module so that the module could be replaced without debugging.

7. Simulation

Figure 16 shows the simulation environment. Simulations were performed using ROS and Gazebo, a 3D model virtual simulator. The environment map was built based on IGVC2022 rules to create an environment similar to the real environment, and the vehicle was designed in the same way as in Orange2022. The simulation allowed us to check the operation of path planning, obstacle avoidance, and debugging without moving the vehicle, understand the causes of errors, and improve and modify the vehicle software. It is necessary to confirm the vehicle's operation to make improvements and corrections. Therefore, confirming possible errors through simulation in advance is an excellent advantage in upgrading the vehicle software.

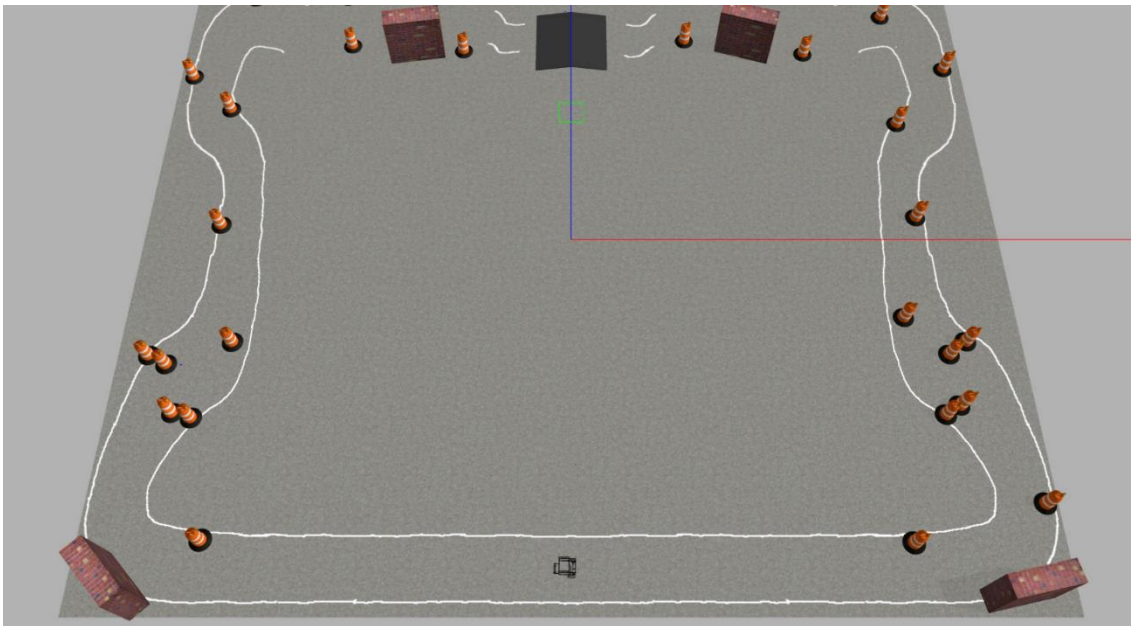


Figure 16. Built simulation environment for IGVC2022

8. Evaluation of Initial Performance

Table 11 shows the expected performance of Orange2022.

Table 11. Performance of Orange2022

Measurement	Performance prediction	Performance result
Speed	6.4km/h(4.0mph)	6.2km/h(3.9mph)
Ramp climbing ability	16.0%incline	15.5%incline
Reaction time	0.22s	0.20s
Battery life	5.0h	4.0h
Obstacle detection distance	0 – 10m(0-33ft)	0 – 10m(0-33ft)
Waypoint navigation	± 0.09m(± 0.30ft)	± 0.09m(± 0.30ft)

9. Conclusion

Based on the failures discovered in Orange2019 and adaptation of the new IGVC2022 rules and guidelines, Orange2022 was designed. In particular, in terms of hardware, we (a) implemented a folding mechanism to enhance the running stability of the vehicle, (b) implemented a suspension mechanism to prevent vehicle tipping when running at the curve, and on the software side, (c) migrated from ROS kinetic to ROS noetic by applying a virtual container approach using Docker. As a result of the implementation of (a), changing the aspect ratio of the vehicle enabled it to run stably even on the curves. In addition, (b) enabled stable autonomous driving by mitigating the impact from the ground and reducing the left-right vibration applied to the vehicle. In addition, (c) used Docker for a seamless transition, automating building and customizing the software installation using a "Dockerfile" to ensure that a consistent build image could be obtained even if the control computer changed. We are confident that Orange2022 yields the best results.

References

¹ IGVC Official Competition Rules (2019), "IGVC 2019 Homepage," <http://www.igvc.org/rules.htm> (accessed January 25, 2019).

² Open Source Robotics Foundation (2019), "ROS Wiki," <http://wiki.ros.org/> (accessed April 10, 2019).